Check for updates

Removal of diclofenac by adsorption process studied in free-base porphyrin Zr-metal organic frameworks (Zr-MOFs)†

Nicholaus Prasetya [ID] * and Christof Wöll [ID]

As the world population continues to grow, there is also a rising concern regarding water pollution since this condition could negatively impact the supply of clean water. One of the most recent concerns is related to the pollution that comes from various pharmaceuticals, in particular non-steroidal anti-inflammatory drugs (NSAIDs) since they have been industrially produced at large scale and can be easily purchased as an over-the-counter medicine. Diclofenac is one of the most popular NSAIDs because of its high-effectiveness, which leads to its excessive consumption. Consequently, its presence in water bodies is also continuously increasing. An adsorption process could then be employed as a highly effective method to address this issue. In comparison to other conventional adsorbents such as activated carbon, the use of metal–organic frameworks (MOFs) as an alternative adsorbent is very attractive since it can offer various advantages such as tailorability and high adsorption capacity. In this study, the performance of three water-stable, free-base porphyrin MOFs assembled using zirconia-based nodes, namely MOF-525, MOF-545, and NU-902, for diclofenac adsorption was thoroughly investigated. Interestingly, although all three free-base porphyrin MOFs are assembled using the same building block and have a similar specific surface area (based on the experimental argon physisorption and calculation based on non-localized density functional theory), their diclofenac adsorption capacity is substantially different from one another. It is found that the highest diclofenac adsorption capacity is shown by MOF-525, which has maximum capacity around 792 mg g^{-1}. This is then followed by MOF-545 and NU-902 that have adsorption capacities around 591 and 486 mg g^{-1}, respectively. Some possible adsorption mechanisms are then thoroughly discussed that might contribute to this phenomenon. Lastly, their performance is also compared with other MOFs that are also studied for this purpose to show their performance superiority not only in terms of adsorption capacity but also their affinity towards the diclofenac molecule, which might be useful as an adsorption performance indicator in the real condition where the contaminant concentration is considerably low.

Introduction

Along with the continual growth of world population comes a rise in concern regarding water pollution resulting from contaminants of emerging concern (CEC).[1] Among the various classes of CECs, the removal of various pharmaceutically active compounds (PhACs) and in particular non-steroidal anti-inflammatory drugs (NSAIDs) from water streams has been intensively investigated. This is because NSAIDs are industrially produced on large scale and are readily available as an over-the-counter medicine. As a consequence, considerable amounts of these efficient drugs are release the surrounding environment

and show unwanted impact, such as growth inhibition towards various organisms[2,3] and inducing genotoxicity and cellular toxicity.[4]

Among various NSAIDs, diclofenac has been considered as the most popular and commonly-used NSAIDs because of its high effectiveness to reduce inflammation and to relieve pain in various disease conditions.[5,6] Despite its proven efficacy, its release to the environment poses serious risks to the surrounding ecosystems. For example, the nephrotoxicity of diclofenac towards *Gyps* vultures in various South Asia countries have been well documented.[7,8] In another study, the toxicity of diclofenac towards *Daphnia magna* as a freshwater crustacean has been reported. In this case, the presence of diclofenac in the water streams has been attributed to a negative impact on gene expression that controls the species' metabolism, growth, development and reproduction.[9] Therefore, it is imperative to effectively remove diclofenac from water streams, ideally until the diclofenac concentration in the water

Institute of Functional Interface (IFG), Karlsruhe Institute of Technology, Hermann-von-Helmholtz-Platz 1, 76344, Eggenstein-Leopoldshafen, Germany. E-mail: nicholaus.prasetya@partner.kit.edu

streams is below the Method Detection Limit (MDL) of 4.74 ng L^{-1},[10] in order to prevent further intoxication of various species.

Addressing the above-mentioned issues, several methods have been proposed to remove diclofenac from water streams, such as ozonation or adsorption to materials like activated sludge.[5] The latter option is preferred, since adsorption processes are highly effective and efficient to remove the unwanted compound without producing toxic byproducts. Consequently, the efficacy of various conventional and new adsorbents such as activated carbon,[11,12] graphene-based materials,[13,14] mesoporous silica,[15,16] and zeolite[17,18] have been investigated to effectively remove diclofenac from water streams.

In the last two decades, there has been a growing interest in a new-class of porous materials, referred to as metal–organic frameworks (MOFs) applied for various purposes.[19–23] As the name suggests, MOFs are a porous crystalline material that is built by stitching metal nodes or clusters with organic ligands the latter colloquially referred to as linkers. MOFs exhibit several attractive properties, such as high surface area, high porosity and the possibility to functionalize the framework in many different ways. Therefore, with regard to removing various PhACs, including diclofenac, MOFs often outperform conventional adsorbents such as activated carbon.[24]

In previous works, the efficacy of MOFs in removing diclofenac from water streams have then been studied by employing different MOFs that are mostly built by using iron (Fe) or zirconium (Zr) as the metal source.[25–27] This is because these high-valence metals can build a strong coordination bonding with the organic ligands, which is crucial in maintaining the framework stability when the MOFs are exposed to water. In this study, we would like to investigate the feasibility of three free-base porphyrins Zr-MOFs to be applied for this purpose. In spite of the fact that there are already a number of reports investigating the use of MOF to remove diclofenac from water streams,[25–31] only few MOFs could achieve a considerably high diclofenac adsorption capacity. For example, the diclofenac adsorption capacity of some well-known MOFs such as UiO-66 [25] and ZIF-8 [30] was reported to be around 200 mg g^{-1}, which is comparable with activated carbons.[24] In addition, some of them also show a relatively slow adsorption kinetic, such as in the case of MIL-100,[31] which means that longer time is required for the adsorption to reach equilibrium. Furthermore, as will be further described in this article, only a few MOFs that have been studied for diclofenac adsorption show a high affinity constant towards diclofenac as indicated by their Langmuir constant and thus could limit its application in the real condition where the diclofenac concentration is relatively low. These three free-base porphyrins Zr-MOFs, namely MOF-525, MOF-545 and NU-902, are chosen because, in addition to their robust framework, they possess high surface area and suitable pore aperture that will enable them to achieve high diclofenac adsorption capacity, fast adsorption kinetic and high diclofenac affinity. However, as will be further discussed below, their similarity in surface area and pore opening does not lead to comparable diclofenac adsorption performance and thus indicating the difference

regarding the interaction strength between the diclofenac and all the free-base porphyrin Zr-MOFs framework. In spite of this, as will also be shown in the last part of the study, these free-base porphyrins Zr-MOFs have successfully exhibited one of the best diclofenac adsorption affinity in comparison to other MOFs which renders them to be very potential in effectively removing the diclofenac molecule from the water streams in the real condition, where the diclofenac concentration is usually very low.

Experimental

Materials

Benzoic acid, 4-methoxybenzoic acid, diclofenac sodium, sodium hydrochloride and zirconyl chloride octahydrate ($ZrOCl_2 \cdot 8H_2O$) were purchased from Merck. *Meso*-tetra(4-carboxyphenyl)porphyrin (H_4TCPP) was purchased from BLD Pharmatech GmbH, Germany. Acetone, dimethylformamide (DMF), hydrochloric acid 37% and formic acid were purchased from VWR Chemicals.

MOF synthesis

Three different MOFs were synthesized during the study, namely: MOF-525, MOF-545 and NU-902. All the MOFs were synthesized using $ZrOCl_2 \cdot 8H_2O$ and H_4TCPP as the metal and ligand source, respectively. However, different modulators were used during the synthesis to obtain pure products. The typical synthesis condition for each MOFs is described below and also schematically given in Fig. 1.

MOF-525. To synthesize pure MOF-525, benzoic acid was used as the modulator following the previous procedure with slight modifications.[32] In a typical synthesis condition, 750 mg of $ZrOCl_2 \cdot 8H_2O$ and 9 g of benzoic acid were firstly dissolved in a Pyrex vial containing 50 mL DMF by sonicating the suspension for about 10 minutes. Once a clear solution was obtained, 250 mg of H_4TCPP was then added and the solution was further sonicated for about 5 minutes to dissolve the ligand. Afterwards, the solution was heated in a convective oven at 100 °C for 24 h. The product was then collected by centrifugation (7000 rpm, 6 minutes) and washed with DMF and acetone. It has been reported that some ligated benzoates could still
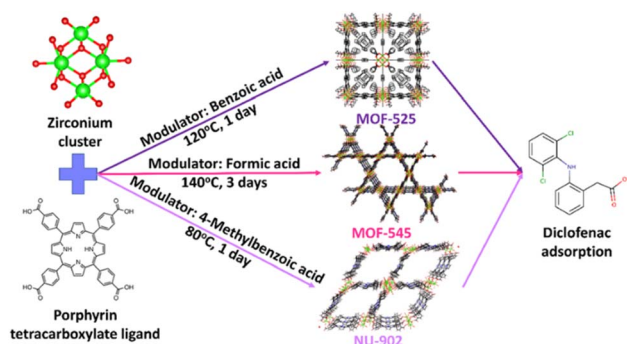

Fig. 1 A schematic of the synthesis condition for MOF-525, MOF-545 and NU-902 applied for diclofenac adsorption.

remain within the framework after the washing process.[33] Therefore, after the washing process, about 200 mg of MOF-525 was immersed in a mixture of 20 mL DMF and 1 mL of 8 M HCl in an oven at 100 °C for 24 h. Afterwards, the product was cooled to room temperature, centrifuged and washed with DMF and acetone. The final product was stored in acetone and heated at 80 °C before being used for adsorption study.

MOF-545. To synthesize pure MOF-545, formic acid was used as the modulator following the previous procedure with a slight modification.[34] In a typical synthesis condition, 750 mg of $ZrOCl_2 \cdot 8H_2O$ and 130 mg of H_4TCPP were dissolved in a Pyrex vial containing a mixture of DMF (200 mL) and formic acid (140 mL). The solution was then sonicated for about 10 minutes to dissolve all the starting materials and placed in a convective oven and heated at 135 °C for 3 days. Afterwards, the product was filtered and washed with DMF and acetone. The product was stored in acetone and was heated at 80 °C overnight before being used for adsorption study.

NU-902. To synthesize pure NU-902, 4-methoxybenzoic acid was used as the modulator following the previous procedure.[35,36] In a typical synthesis condition, 52 mg of $ZrOCl_2 \cdot 8H_2O$ and 200 mg of H_4TCPP were dissolved in a Pyrex vial containing 60 mL DMF with the aid of ultrasonication. Afterwards, 3 g of 4-methoxybenzoic acid was added and the solution was further sonicated for about 2 minutes to dissolve all the starting materials. The solution was then placed in a convective oven and heated at 80 °C for 24 h. Once the reaction finished, the product was collected by centrifugation (7000 rpm, 6 minutes) and washed with DMF. The product was then further washed by dispersing it inside a mixture of 20 mL DMF and 1 mL of 8 M HCl and placed inside a convective oven at 80 °C for 24 h. Afterwards, the product was cooled to room temperature, centrifuged and washed with DMF and acetone. The product was stored in acetone and was heated at 80 °C before being used for adsorption study.

Diclofenac adsorption study

The diclofenac adsorption studies were conducted following previously reported procedures.[28,29] First, a diclofenac stock solution with a concentration of 1 mg mL^{-1} was prepared. For the study of diclofenac adsorption isotherm, a number of diclofenac solutions with different concentration were firstly prepared by diluting the stock solution. The MOFs were then added to the solution and the suspension were sonicated for about 30 s. The MOF dosage for this investigation was set to be 100 mg L^{-1} afterwards, the suspensions were placed on a shaker and left for 48 h to achieve the adsorption equilibrium. Once the adsorption process finished, the concentration of the diclofenac in the supernatant was measured by using UV-Vis spectroscopy.

Meanwhile, for the study of the adsorption kinetics, the stock solution was diluted to obtain a diclofenac solution with a concentration of 10 mg L^{-1}. The MOF adsorbent dosage for this investigation was set to be 10 mg L^{-1}. The concentration of the diclofenac in the solution was then measured at a certain period of time (1, 2, 5, 15, 30, 45, 60, 120, 240, 420 minutes) by employing UV-Vis spectroscopy.

In addition, the effect of temperature and pH on the diclofenac uptake by the MOFs was investigated. In this study, the diclofenac solution concentration and the adsorbent dosage were set to be 50 mg mL^{-1} and 100 mg L^{-1}, respectively. Either 0.1 M HCl or 0.1 M NaOH were carefully added to the diclofenac solution to control the pH. Four different temperatures and five different pH were used during the study, namely 5 °C, 25 °C, 45 °C and 60 °C and pH 5–9.

The possibility to regenerate the loaded MOFs was investigated by washing with a mixture of methanol/acetic acid (9 : 1) after the diclofenac adsorption process took place. After washing, the adsorbents were dried at 80 °C before being used for another adsorption cycle.

Characterizations

Powder X-ray diffraction. The powder X-ray diffraction (PXRD) pattern of the samples were collected by using a D8 A25 Da-Vinci Bruker XRD. The samples were measured between 2θ 2–20°.

Fourier-transformed infrared spectroscopy. The Fourier-transform infrared (FTIR) spectra of the samples were recorded by using Bruker Hyperion – Tensor in Attenuated Total Reflectance (ATR) mode. The measurement took place between the wavenumber 4000–400 cm^{-1}. Meanwhile, the difference FTIR spectra of the MOFs after the adsorption and regeneration process was obtained by subtracting the FTIR spectra of the MOFs after the adsorption and regeneration process by the pristine MOFs before the adsorption process took place.

Argon physisorption. The BET values of the synthesized MOFs were determined *via* argon physisorption using an Autosorb Quantachrome instrument. Before the measurement took place, the MOF samples were activated by heating them under vacuum at 75 °C for 24 h.

UV-Vis spectroscopy. To determine the diclofenac concentration in the solutions, the absorbance value of the solutions at 276 nm was recorded by using Cary 5000 UV/Vis Spectrophotometer equipped with Cary Universal Measurement Accessory (UMA).

Results and discussions

MOF synthesis and characterizations

As has been previously stated, three different MOFs were investigated during this study: MOF-525, MOF-545 and NU-902. These MOFs have considerably high surface area and suitable pore aperture that might be suitable to effectively remove diclofenac from water streams.[37] According to the previous report,[33] all the three free-base porphyrins Zr-MOFs could actually be synthesized by using the same metal source (zirconyl chloride octahydrate) and modulator (benzoic acid). However, the reaction or each MOF synthesis had to be carried out at different temperatures. In our investigation, however, we found that the most reproducible technique to obtain the pure products of these free-base porphyrins Zr-MOFs is not only dependent on adjusting the reaction temperature but also on using the correct modulator. For example, our attempt to produce NU-

902 MOF with using benzoic acid as the modulator but at lower temperature than MOF-525 synthesis did not yield a pure NU-902 product. As can be seen in the ESI Fig. S1,† the MOF synthesized using this approach was likely a mixture of MOF-525 and NU-902 since the PXRD pattern resembles both the pattern of MOF-525 and NU-902. Such a phase mixture product of free-base porphyrins Zr-MOFs is then a phenomenon that is not uncommon to be encountered and the synthesis condition must thus be optimized to obtain a pure phase product.[37–39] Therefore, benzoic acid, formic acid and 4-methoxybenzoic acid were chosen in our study as the most suitable modulator to reproducibly synthesize pure MOF-525, MOF-545 and NU-902, respectively.

The purity and crystallinity of the MOFs synthesized in this study are determined from their PXRD pattern. From Fig. 2(A), it can be seen that PXRD patterns of all the MOFs are in line with the corresponding calculated patterns, no unidentified peaks were present. This observation reveals the high purity of the products and the efficacy of using different modulators in controlling the final framework topology of the free-base porphyrins Zr-MOFs. The FTIR spectrum of all free-base porphyrins Zr-MOFs studied here are presented in Fig. 2(B). As expected, all the three free-base porphyrins Zr-MOFs show identical FTIR spectra since they are built with the same building block despite the fact that their framework topology is different from each other. In this respect, one of the most prominent peaks shown by all the free-base porphyrins Zr-MOFs is the peak around 1600, 1410 and 660 cm^{-1}, which corresponds to the asymmetric and symmetric stretching of carboxylate linker and stretching mode of metal–ligand bonding, respectively, in the Zr-porphyrin MOF.[40] In addition to the PXRD and FTIR, the UV-Vis spectra of the digested samples of the as-synthesized free-base porphyrins Zr-MOFs were also recorded and the result is presented in Fig. 2(C). This characterization is particularly important to check whether metalation process occurs during the MOF synthesis. In this case, there is a possibility that the porphyrin ligand might be metalated with Zr during the MOF synthesis, as is the case for other MOFs synthesized using solvothermal methods at elevated temperatures.[41] However, as can be seen from the result, such a spontaneous metalation process did not occur during the synthesis since the UV-Vis spectra of all the digested free-base porphyrins Zr-MOFs are identical with the free-base porphyrin ligand. Therefore, it is safe to conclude that all the free-base porphyrins Zr-MOFs used in this study are metal-free free-base porphyrins Zr-MOFs assembled using zirconia-based nodes.

The porosity of the MOFs was then evaluated by analyzing their surface area through argon physisorption and the result is given in Fig. 3(A). Theoretical surface area values for MOF-525, MOF-545, and NU-902 were obtained using the non-localized density functional theory (NLDFT) cylindrical pore method and were found to amount to 1955, 1998 and 1912 m^2 g^{-1}, respectively. Meanwhile, the pore size distribution, which is also estimated based on the same method (NLDFT), for all the free-base porphyrins Zr-MOFs is given in Fig. 3(B). It can be seen from the result that the pore size distribution of all the free-base porphyrins Zr-MOFs peaks at around 1.5–2 nm. Such a pore
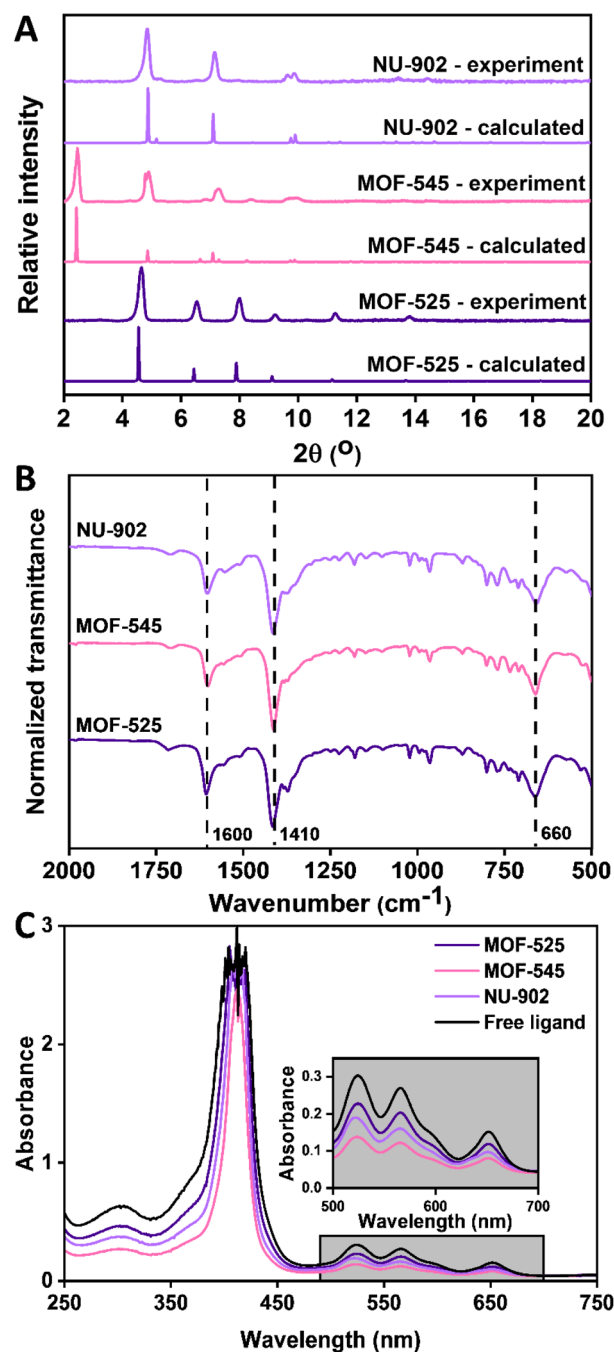

Fig. 2 PXRD pattern (A), FTIR spectra (B) and the UV–Vis spectra of the digested samples (C) of MOF–525, MOF–545 and NU–902 synthesized in this study.

opening should be large enough for the diclofenac molecule to enter the framework.

Diclofenac adsorption study of free-base porphyrin Zr-MOFs

Having successfully obtained and fully characterized pure MOF-525, MOF-545, and NU-902, we then proceeded to investigate their diclofenac adsorption performance. We first studied the diclofenac adsorption kinetics in MOF-525, MOF-545, and NU-902. The results are given in Fig. 4. From the figure, it can be
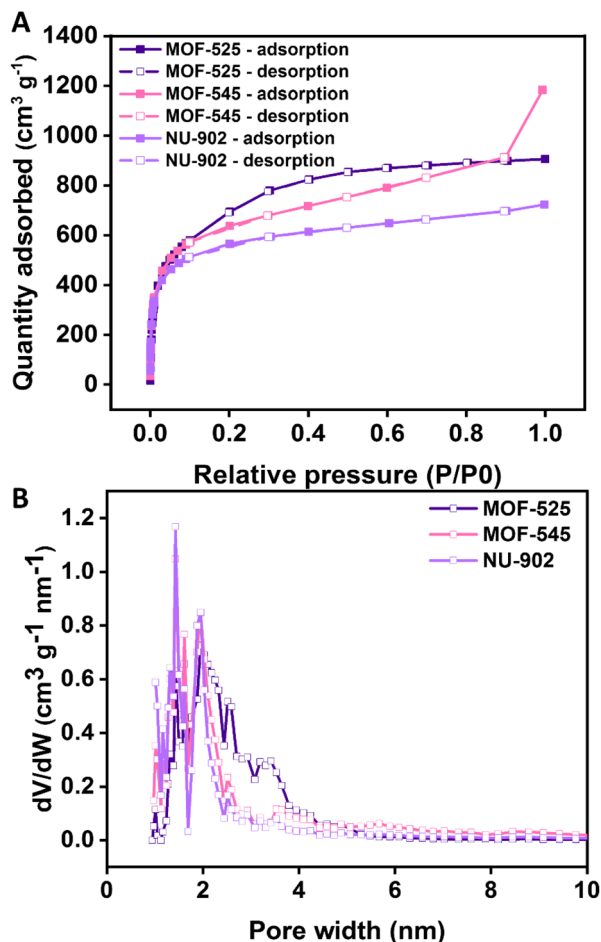
Fig. 3 Argon physisorption (A) and pore size distribution (B) based on NLDFT of MOF–525, MOF–545 and NU–902.

seen that MOF-525 and NU-902 have the highest and lowest diclofenac adsorption capacity, respectively. We then analyze the kinetic data by fitting it using the pseudo-first-order (PFO)
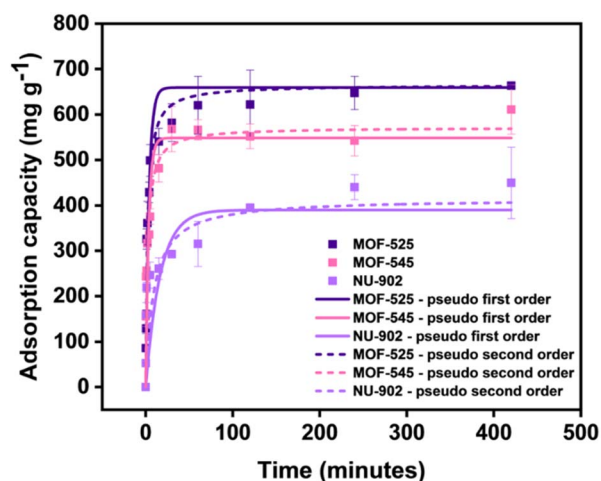

Fig. 4 Comparison of diclofenac adsorption isotherms for MOF–525, MOF–545, and NU–902 with the corresponding fits using first and second order kinetic models.

and pseudo-second-order (PSO) model[42] and the results for the parameter value are presented in Table 1. From the result, it can be seen that the diclofenac adsorption kinetic in all the MOFs can be fitted well both with PFO and PSO model, although PSO is slightly better in this case considering its slightly higher coefficient of determination. From the PSO model, the adsorption equilibrium capacity of MOF-522, MOF-545 and NU-902 is found to be around 665, 571 and 415 mg g^{-1}. Similar values are also obtained when the kinetic data were fitted with PFO model. Further analysis based on the PSO model also shows that the kinetic constant of both MOF-525 and MOF-545 is almost three times higher than in NU-902. This then indicates that the diclofenac adsorption process in both MOF-525 and MOF-545 occurs much faster than in NU-902. Despite this, more than 90% of adsorption equilibrium can be reached by all free-base porphyrins Zr-MOFs in less than 1 hour. This performance is considerably faster if one compares with other MOFs such as UiO-66-(COOH)$_2$[43] and MIL-100(Fe)[31] that require around 20 hours to achieve the comparable performance.

The adsorption kinetic data was then further analyzed to obtain an insight regarding the rate-controlling step governing the adsorption process. During the adsorption process, two steps will usually occur before the adsorbate gets adsorbed unto the adsorbent's surface.[44,45] Firstly, the adsorbate will diffuse from the bulk solution to the surface of the adsorbent. This step is usually called film-diffusion. Afterwards, the diffusion process of the adsorbate within the adsorbents' pores occurs before the adsorbate gets adsorbed on the adsorbents' surface. This step is usually called intra-particle diffusion. Either the film diffusion, intra-particle diffusion or the combination of both could be the rate-determining step of the adsorption process. If one of the diffusion processes is more significant than the other, the whole mass-transfer process could be simplified based on it as the rate-controlling step.

In this study, four models, which assume that either film diffusion or intra-particle diffusion acts as the rate-controlling step during the adsorption process, are then selected to further analyze the diclofenac adsorption process in the free-base porphyrins Zr-MOFs. The result for this analysis is presented in Fig. 5. If the adsorption process is governed by the film-diffusion process, a linear relationship should appear in the Fig. 5(A) and (B), which are based on the study of Yao and

Table 1 The parameters values of pseudo first order (PFO) and pseudo second order (PSO) model fitted for diclofenac adsorption of MOF–525, MOF–545 and NU–902

Parameter	MOF-525	MOF-545	NU-902
Pseudo First Order (PFO)			
q (mg g^{-1})	659	548	390
k_1 (min^{-1})	0.2653	0.2998	0.06007
R^2	0.99992	1	0.00035
Pseudo second order (PSO)			
q (mg g^{-1})	665	571	415
k_2 (mg g^{-1} min^{-1})	7.06×10^{-4}	7.97×10^{-4}	2.64×10^{-4}
R^2	0.99998	1	0.99962

Chen[44] and Boyd and co-workers.[46] Meanwhile, in the case where the intra-particle diffusion controls the adsorption process, both Fig. 5(C) and (D), which are based on the intra-particle diffusion from Weber and Morris[47] and Boyd[46] model, respectively, should give a linear relationship and pass through the origin.[44] However, from the results, it can be seen that neither of these models gives a linear relationship for all the free-base porphyrins Zr-MOFs.

Considering the system was homogeneously agitated during the adsorption process, one could then assume that the film diffusion should not control the adsorption process because the agitation would eliminate the concentration gradient on the surface of the MOF. However, it should also be noted that the film diffusion process could also be contributed by the presence of a surface barrier on the surface of a MOF. Such a surface barrier can be caused by various factors such as the presence of impurities or imperfection on the MOF's surface.[48] Surface barriers might also contribute in slowing down the adsorption kinetic because it acts as an additional resistance before an adsorbate could get into the MOF's pores. In this respect, it could be seen that, since the film diffusion is not the rate-limiting step during the adsorption process, the contribution of the surface barrier in all the free-base porphyrins Zr-MOFs might not be very significant. However, this does not necessarily mean that the surface of all the free-base porphyrins Zr-MOFs used in this study is perfect and thus containing no impurities. This is because it could also be the case that the contribution of the surface barrier that might exist on the surface of the free-base porphyrins Zr-MOFs are not big enough to give additional resistance so that it can control the whole adsorption process. Therefore, in this case, the existence of the surface barrier on the free-base porphyrins Zr-MOFs is then neither confirmed nor eliminated. In addition, considering the relatively big pore aperture of the free-base porphyrins Zr-MOFs, the intra-particle diffusion should also not be the rate-controlling step since the diclofenac molecule should be able to move freely within the pores of the free-base porphyrins Zr-MOFs. In this case, it could then be concluded that neither film diffusion nor intra-particle diffusion controls the diclofenac adsorption process in MOF-525, MOF-545 and NU-902.

Having studied the diclofenac adsorption kinetic, we then investigated the diclofenac adsorption isotherm for all the MOFs. The result for this study is given in Fig. 6 and its adsorption isotherm parameter value is shown in Table 2. As also in the case of kinetic adsorption study, it can be seen that the diclofenac adsorption capacity of the MOFs used in this study follows in the order of MOF-525, MOF-545 and NU-902. Both Langmuir and Freundlich model seem also sufficient to fit the diclofenac adsorption in all free-base porphyrins Zr-MOFs. Based on the Langmuir isotherm, the maximum diclofenac adsorption capacity of MOF-525, MOF-545 and NU-902 is found to be around 792, 591 and 486 mg g^{-1}, respectively. The maximum diclofenac uptake obtained by Langmuir isotherm that is exhibited by MOF-525 is also one of the highest values observed for MOF-based materials. Previously, a similar high uptake was also observed in MOF-808 whose maximum diclofenac uptake was found to be around 833 mg g^{-1}.[28] Combined with a relatively fast adsorption kinetic, MOF-525 could then be another promising potential to be applied as an adsorbent to remove diclofenac from the water streams.

The impact of pH on the diclofenac adsorption of MOF-525, MOF-545 and NU-902 was also studied and the result is presented in Fig. 7(A). Regarding the impact of pH, it can be observed that change of pH between 5 and 9 during the experiment only impart a slight impact on the diclofenac adsorption capacity for all the MOFs used in this study. However, a tendency can also actually be seen that an optimum pH, namely between 6 and 7, does exist where all the free-base porphyrins Zr-MOFs show the highest diclofenac adsorption capacity. Either an increase or a decrease of the pH will then result in a slight decrease in the adsorption capacity. Such a phenomenon has also been previously observed in other MOF-based adsorbents, which could be associated with various
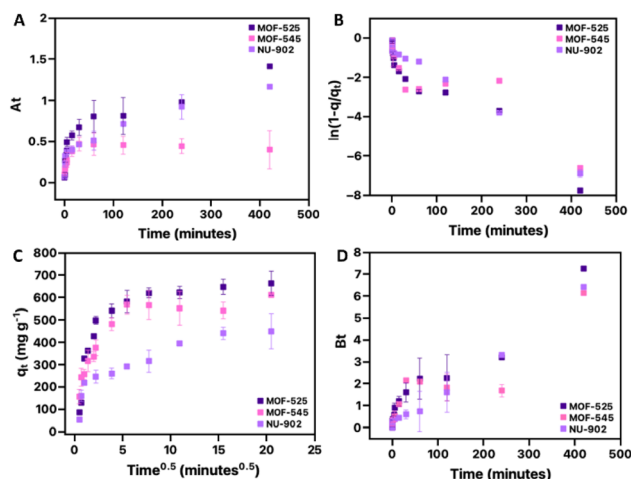

Fig. 5 The analyses on the diclofenac adsorption kinetic of MOF-525, MOF-545 and NU-902 based on film-diffusion (A and B) and intra-particle diffusion (C and D) as the rate-controlling step.
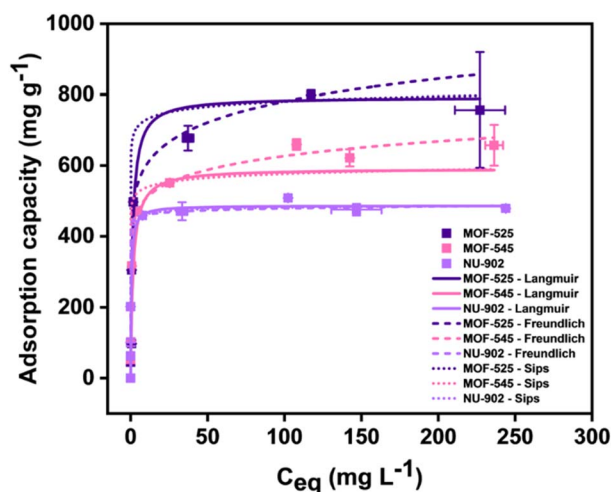

Fig. 6 The diclofenac adsorption isotherm of MOF-525, MOF-545 and NU-902 with their corresponding fitted models.

Table 2 The parameters values of Langmuir, Freundlich and Sips model fitted for diclofenac adsorption of MOF-525, MOF-545 and NU-902

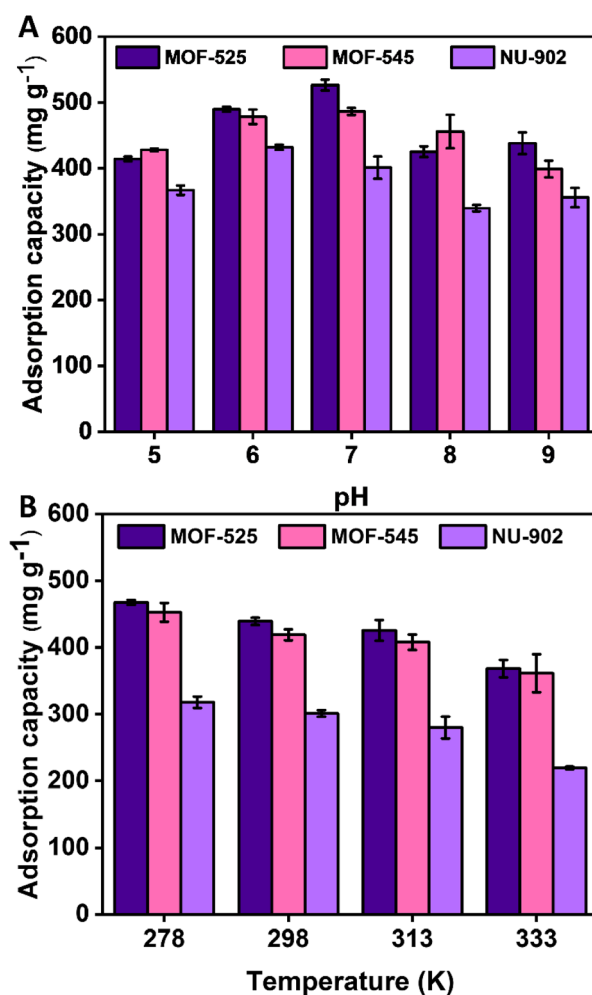| Parameter	MOF-525	MOF-545	NU-902
Langmuir			
q_{max} (mg g^{-1})	792	591	486
K_L	0.75	0.62	2.17
R^2	0.99996	0.99996	0.99999
Freundlich			
K_F	461.56	409.76	444.4
n	8.76	10.83	61.3
R^2	0.99999	0.99999	0.99999
Sips			
q_{max} (mg g^{-1})	976	776	496
K_{Sips}	392.8	195.3	100
N	0.131	0.107	0.38
R^2	0.98325	0.99625	0.99999

factors particularly the increasing negative impact from electrostatic repulsion when the pH is increased.[49] Meanwhile, when the pH solution is decreased, there might be a possibility that some of the diclofenac molecules precipitate from the solution. As a consequence, less diclofenac molecules are available in the solution to be adsorbed by the MOFs resulting in a reduced adsorption capacity.

Meanwhile the effect of temperature on the diclofenac adsorption for all the free-base porphyrins Zr-MOFs used in this study is given in Fig. 7(B). Differing from the impact of pH, the trend of diclofenac adsorption in this case is more obvious. From the result, it can be seen that higher operating temperature results in lower diclofenac adsorption capacity for all the free-base porphyrins Zr-MOFs. This then indicates that the diclofenac adsorption in the MOFs is an exothermic process. Such a trend has also previously been observed in other MOFs for diclofenac adsorption such as MOF-801 (ref. 29) and MOF-808.[28]

The thermodynamic parameters are also evaluated and the result is given in Table 3. As has been previously stated, the ΔH of the adsorption process for all the MOFs are all negative and thus indicating an exothermic process. The value of the adsorption enthalpy also follows the order of the diclofenac adsorption capacity of the MOFs, namely MOF-525, MOF-545, and NU-902. The entropy of the adsorption process for all the free-base porphyrins Zr-MOFs is found to be negative. This might then indicate the reduction of the disorder of the diclofenac molecule during the adsorption process. In this case, once being adsorbed, the diclofenac molecule might no longer be able to move freely as in the case when they are in the solution. Lastly, it can also be seen that the diclofenac adsorption process in all the MOFs at different operating temperatures occur spontaneously as indicated by the negative value of ΔG.

Having experimentally conducting the diclofenac adsorption on all the free-base porphyrins Zr-MOFs, we then try to elucidate the various factors that might influence the diclofenac adsorption performance in the free-base porphyrins Zr-MOFs. Firstly,

the PXRD pattern of the MOF after the diclofenac adsorption was recorded and the result is presented in Fig. 8(A). From the result, it can be seen that, although the presence of the majority of the peaks are still obvious, their relative intensities are substantially different from the freshly-activated MOFs before being used for adsorption. This phenomenon was also previously observed when investigating the applicability of surface-mounted MOFs (SURMOFs) for photonic antenna processes.[50] In the study, after the HKUST-1 SURMOF was loaded with Eu(bzac$_3$)bipy (bzac = 1-benzoylacetone, bipy = 2,2′-bipyridine) molecule, a pronounced difference in the relative intensities of the XRD pattern in comparison to the pristine HKUST-1 SURMOF was observed. This change in form factor is a result from the strong increase in electron density by loading a metal-containing compound into every pore of the MOF. In the current case, the changes of the relative intensities of PXRD peaks after the adsorption process are related to the presence of diclofenac guests within the pores of the free-base porphyrins Zr-MOFs. These changes in the PXRD pattern thus clearly reveal that the diclofenac molecules are not only adsorbed on the outer surfaces of the MOF particles but must also have been

Fig. 7 The effect of pH (A) and temperature (B) on the diclofenac adsorption of MOF-525, MOF-545 and NU-902.

Table 3 Thermodynamic parameters value of MOF-525, MOF-545, and NU-902 during the diclofenac adsorption process

Parameter	MOF-525	MOF-545	NU-902
ΔH (kJ mol^{-1})	−21.34	−16.98	−10.82
ΔS (J^{-1} K^{-1})	−35.92	−23.78	−14.47
ΔG_{278} (kJ mol^{-1})	−11.35	−10.37	−6.79
ΔG_{298} (kJ mol^{-1})	−10.63	−9.89	−6.5
ΔG_{313} (kJ mol^{-1})	−10.09	−9.54	−6.28
ΔG_{333} (kJ mol^{-1})	−9.38	−9.07	−6

loaded into the pores. A simple adsorption of these pharmaceutical model compound to the water/MOF interface would not lead to changes in the relative intensities within the PXRD patterns.

This is also confirmed by the FTIR spectra of the free-base porphyrins Zr-MOFs after the adsorption process. From the Fig. 8(B), and more prominently from Fig. 8(C) where the difference FTIR spectra of all free-base porphyrins Zr-MOFs after and before diclofenac adsorption is computed, it can be seen that some peaks belonging to diclofenac molecule appear in the spectra of the free-base porphyrins Zr-MOFs after they are being used for adsorption. For example, the peaks at around 1450 cm^{-1} and 1500 cm^{-1} could be associated with the symmetric and asymmetric stretching, respectively, from the carboxylate group of the diclofenac molecule.[51] Meanwhile, the stretching mode of C–Cl in the diclofenac molecule could be indicated by the appearance of the peak around 636 cm^{-1}. Lastly, the presence of diclofenac in all the Zr–porphyrin can also be corroborated by observing the UV-Vis spectra of the digested samples, as presented in the Fig. 8(D). From the spectra, it can be seen that a new peak at around 275 nm appears after all the MOFs were used for diclofenac adsorption and thus clearly indicating the existence of the diclofenac molecule in all the free-base porphyrins Zr-MOFs.
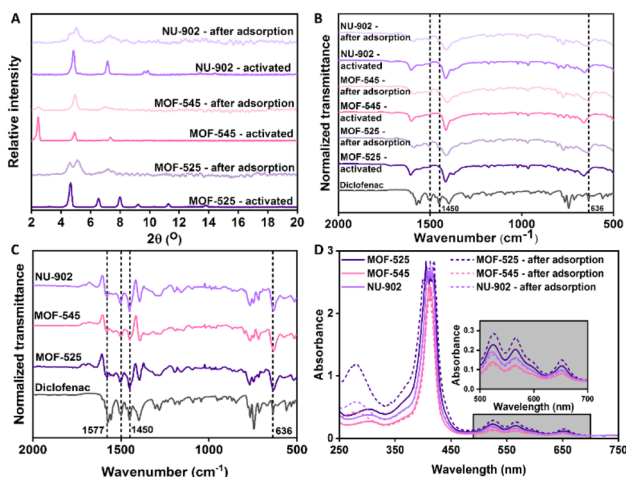
From these analyses, it can then be safely inferred that the diclofenac molecule actually goes inside the pore of all the free-base porphyrins Zr-MOFs to access their available surface area for adsorption. Generally, when there are no special adsorption sites in an adsorbent, the trend of an adsorption capacity should be predominantly influenced by the surface area that is available and accessible for adsorption.[25] Therefore, an adsorbent with higher surface area usually exhibits higher adsorption capacity. However, as has been previously shown, such a trend is not observed in this study although it can be seen from the characterization results that all the free-base porphyrins Zr-MOFs have similar surface area, namely around 2000 m^2 g^{-1}. When the diclofenac adsorption capacity for all the free-base porphyrins Zr-MOFs is normalized against the surface area, it becomes clearer that MOF-525 has the highest value at around 0.41 mg m^{-2} and is followed by MOF-545 and NU-902, whose normalized diclofenac adsorption capacity is found to be around 0.29 and 0.25 mg m^{-2}, respectively. Therefore, in this case, there are also other factors that influence the diclofenac adsorption performance in the free-base porphyrins Zr-MOFs apart from their surface area.

In this case, it could be firstly hypothesized that the porphyrin ligand in some of the free-base porphyrins Zr-MOFs might be metalated during the adsorption process and thus could significantly affect their adsorption performance by manipulating the framework interaction with the diclofenac molecule. Although the initial characterization has clearly shown that the porphyrin ligand in all free-base porphyrins Zr-MOFs was metal-free, the likelihood might come from the use of diclofenac sodium as the source of diclofenac during the adsorption study and thus the porphyrin ligand might be metalated with sodium. However, the possibility of the existence of such an interaction in all free-base porphyrins Zr-MOFs could be excluded by also observing UV-Vis spectra of all the digested free-base porphyrins Zr-MOFs as given in Fig. 8(D). In addition to give an indication regarding the presence of diclofenac in the MOFs, one can clearly observe that the UV-Vis spectra, particularly in the wavelength range between 500 and 700 nm, of all free-base porphyrins Zr-MOFs after diclofenac adsorption are identical with the UV-Vis spectra before adsorption. This then clearly indicates that the metalation process did not occur during the diclofenac adsorption and the porphyrin center of all the free-base porphyrins Zr-MOFs remained metal-free.

Therefore, to better elucidate other different interaction possibilities between the diclofenac molecule and the free-base porphyrins Zr-MOFs, the PXRD pattern, FTIR spectra and the UV-Vis spectra of the digested samples of MOF-525, MOF-545 and NU-902 after being washed with a mixture of methanol and acetic acid were also collected and shown in Fig. 9(A), (B) and (C) respectively. Firstly, it can be clearly seen from the Fig. 9(A) that there is only a slight change regarding the PXRD pattern of all free-base porphyrins Zr-MOFs after the regeneration process took place, particularly for MOF-525 and MOF-545. This might then firstly indicate that the crystal structure of both MOF-525 and MOF-545 are not significantly altered after the adsorption process. However, a slightly contrasting situation
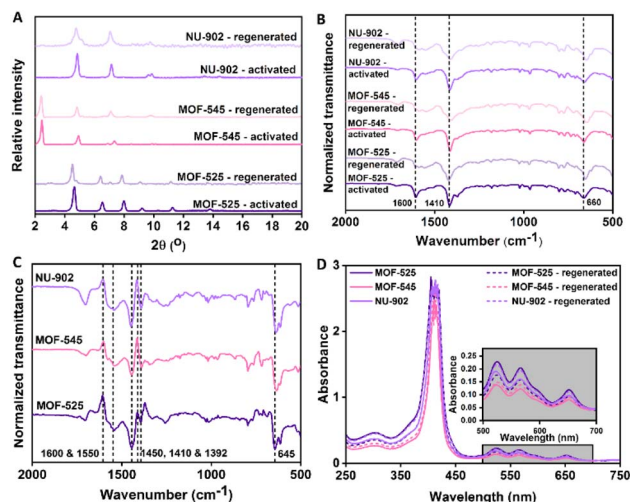

Fig. 8 The PXRD pattern (A), FTIR spectra (B), difference FTIR spectra before and after adsorption (C) and UV-Vis spectra of the digested samples (D) of MOF-525, MOF-545 and NU-902 after adsorbing diclofenac molecule.

Fig. 9 The PXRD pattern (A), FTIR spectra (B), difference FTIR spectra before adsorption and after regeneration (C) and UV–Vis spectra of the digested samples (D) of regenerated MOF-525, MOF-545 and NU-902 after completing diclofenac adsorption.

can be seen in the case of NU-902. In comparison to MOF-525 and MOF-545, the change in PXRD pattern after regeneration process is more prominent. Therefore, it could be hypothesized that the adsorption of the diclofenac molecule has more impacts on the crystal structure of NU-902 rather than on MOF-525 and MOF-545.

However, a different situation can be observed on the FTIR spectra of all free-base porphyrins Zr-MOFs after the regeneration process as shown in Fig. 9(B). In this case, the change in the IR spectra of all free-base porphyrins Zr-MOFs after the regeneration process took place is more prominent in comparison to the activated samples. In particular, it can be seen that the peak at wavenumber around 660 cm^{-1} is slightly red-shifted in comparison to the activated samples. As can be seen from the difference FTIR spectra in Fig. 9(C) of all free-base porphyrins Zr-MOFs after regeneration process and activated samples, it can be seen that this particular peak now appears at around wavenumber 640 cm^{-1}. Such a change is more prominently observed in the case of NU-902 and MOF-545 than in MOF-525, since the peak red-shifting of the later is less pronounced than the formers. Since this peak could be associated with the metal–ligand bonding of the free-base porphyrins Zr-MOFs, this shift might then indicate the alteration of the coordination bonding environment experienced in all the free-base porphyrin MOFs. This is further corroborated if one looks closer to the peak at wavenumber around 1600 cm^{-1} and 1410 cm^{-1}, which could be associated with the asymmetric and symmetric stretching of carboxylate group, respectively, and are responsible in building a coordination bonding with the Zr-metal cluster. As can be seen in Fig. 9(B), both peaks in all the regenerated free-base porphyrins Zr-MOFs are broadened in comparison to the activated samples and thus indicating the alteration of the coordination bonding environment. A closer look on the difference spectra as given in Fig. 9(C) also indicates that the normalized transmittance of both peaks in all the regenerated free-base

porphyrins Zr-MOFs is lower in comparison to the activated samples. Moreover, both peaks might also be red-shifted as indicated by the increase intensity of the peak at around 1550 cm^{-1} and 1392 cm^{-1}, respectively.

On the basis of these observation, we hypothesized that in addition to adsorption mechanisms that only involve electrostatic and hydrophobic interaction, other adsorption mechanisms that affect the coordination bonding environment in the free-base porphyrins Zr-MOFs might also have an important role during for the diclofenac adsorption process. We see two mechanism possibilities where the coordination bonding environment between the ligand and the metal cluster could be affected: a hydrogen bonding between the diclofenac molecule and the carboxylate group of the porphyrin and the establishment of coordination bonding between the diclofenac molecule and the Zr-metal cluster could also not be excluded. Moreover, these bonding could also contribute in building a relatively strong interaction between the diclofenac molecule and all the free-base porphyrins Zr-MOFs resulting in an ineffective removal of the adsorbed diclofenac from all the free-base porphyrins Zr-MOFs framework even after the regeneration takes place. Although as can be seen in Fig. 9(D) that the peak belonging to diclofenac can no longer be observed in the UV–Vis spectra of all digested free-base porphyrins Zr-MOFs, the difference FTIR spectra as given in Fig. 9(C) might still suggest the existence of the diclofenac molecule inside all the Zr–porphyrin MOF framework as indicated by the presence of the peak at wavenumber around 1450 cm^{-1}. Consequently, this situation might then render persisting changes and impacts to the framework environment of all the free-base porphyrins Zr-MOFs as suggested by the change of the PXRD pattern and FTIR spectra of all regenerated samples. In this case, it could be further argued that the impact of both interactions is larger in NU-902 rather than in MOF-525 and MOF-545. This is because the regenerated NU-902 with **scu** topology exhibits the most prominent change both in the PXRD pattern and FTIR spectrum. Meanwhile, while also considering from the change of the PXRD pattern and FTIR spectrum, MOF-525 with **ftw** topology arguably experiences the least impact in this case.

Such a situation might also partially explain the reason why MOF-525 has the highest diclofenac adsorption uptake per (theoretically) available surface area. In this case, it could be argued that the role of both hydrogen bonding and coordination bonding between the diclofenac molecule and MOF-525 is the least significant in comparison to MOF-545 and NU-902. Therefore, the diclofenac molecule could utilize the available and accessible surface area of MOF-525 to get adsorbed. In contrast, these impacts are felt greatest in NU-902. In this case, the diclofenac molecule could probably be more accumulated in the area of the NU-902 metal cluster, where coordination bonding and hydrogen bonding could possibly occur. Such an aggregation might then lead to inefficient utilization of the available surface area of NU-902 for the adsorption process because of the limitation of the available metal cluster sites for adsorption and the possibility to block the pore aperture of NU-902 so the rest of the diclofenac molecule could not access the available surface area.

Table 4 The comparison of diclofenac adsorption performance of various MOFs–based porous materials

MOF	Maximum adsorption capacity[a] (q_{max}, mg g^{-1})	Langmuir constant[a] (K_L, L mg^{-1})	Diclofenac affinity ($q_{max} \times K_L$, L g^{-1})	Ref.
MIL-53(Al)	422	0.0598	25.2	52
MIL-100(Fe)	357	n.a	—	26
Sulfonic-functionalized MIL-100(Fe)	476	n.a	—	
MIL-100(Fe)	773	0.0268	20.7	31
MOF-808	833	0.36	299.8	28
MOF-801	173	0.052	8.9	29
Defective-MOF-801	680	0.154	104.7	
Fe$_3$O$_4$@MOF-100(Fe)	377	0.48	181.1	49
UiO-66	189	0.039	7.4	25
UiO-66-NH$_2$	106	0.069	7.3	
UiO-66-18%SO$_3$H	263	0.008	2.1	
UiO-66-(COOH)$_2$	480	0.053	25.4	43
UiO-66-(COOCu)$_2$	624	0.087	54.3	
UiO-66(COOFe)$_2$	769	0.049	37.7	
UiO-66-NH$_2$	555	0.0689	38.2	27
ZIF-8-derived porous carbon	400	0.22	88	30
ZIF-8	100	0.042	4.2	
MOF-525	792	0.75	594	This work
MOF-545	591	0.62	366.4	
NU-902	486	2.17	1054.6	

[a] The values are based on the fitting of Langmuir equation and the adsorption process was conducted at room temperature without pH adjustment.

Having fully discussed the performance of all the free-base porphyrins Zr-MOFs for the diclofenac adsorption and their possible adsorption mechanisms, their performance is also compared with other MOF-based porous materials that have been studied to perform the same task and given in Table 4. Such a comparison study is important to locate the position of the free-base porphyrins Zr-MOFs to perform this task.

Zr-MOFs, particularly MOF-525 and MOF-545, used in this study has better diclofenac adsorption capacity than most of the studied MOFs-based porous material. Interestingly, all the free-base porphyrins Zr-MOFs does not only show a high diclofenac adsorption capacity but also high affinity towards this molecule. This is exhibited by the relatively higher value of diclofenac affinity of the free-base porphyrins Zr-MOFs than the rest of the MOFs-based porous materials. For example, although the maximum adsorption capacity of UiO-66(COOFe)$_2$ is found to be comparable with MOF-525,[43] the affinity value of the former is one order of magnitude lower than the latter. Taking into account this affinity value could be considered more important than just merely looking into the maximum adsorption capacity since, in the real case where these adsorbents are going to be deployed in the water streams, the concentration of the contaminants will be considerably lower than the concentration used during the study and this affinity value will reflect the capability of the materials to retain its adsorption capability within in this condition.[24] From the analysis of this affinity, it can also be seen that, although NU-902 has the lowest maximum diclofenac adsorption capacity in comparison to MOF-525 and MOF-545, its diclofenac affinity is calculated to be the highest and therefore could indicate its suitability to be deployed in the real conditions. Moreover, even though all these free-base porphyrin Zr-MOFs have strong affinity towards

diclofenac, the diclofenac molecules could still be effectively desorbed through a simple regeneration process by washing the MOFs with solvents. As can be seen in the Fig. S3 in the ESI,† the adsorption capacity of all these MOFs could be well retained for at least three adsorption cycles before a slight decrease is observed in the fourth cycle which might indicate the exhaustion. Despite this, their diclofenac adsorption capacity could still be well maintained around 70–80% of their maximum adsorption capacity and thus still clearly demonstrating a good adsorption capability.

Conclusions

In conclusion, three different free-base porphyrins Zr-MOFs incorporating zirconia-based nodes with different topologies, namely MOF-525, MOF-545 and NU-902, have been successfully synthesized in this study by carefully adjusting their reaction conditions and using the right modulator. The diclofenac adsorption performance of the resulting material was then investigated. In general, all the three free-base porphyrins Zr-MOFs were found to exhibit good diclofenac adsorption capacity, which falls in the range of 480–800 mg g^{-1}. It was found that the highest and lowest diclofenac adsorption capacity is owned by MOF-525 and NU-902, respectively. In this case, various adsorption mechanisms might be involved but arguably, the difference in the adsorption uptake between the three free-base porphyrins Zr-MOFs is heavily influenced by the hydrogen bonding and coordination bonding established between the diclofenac and the MOF framework. Despite this, all the three porphyrinic MOFs show good diclofenac adsorption performance when compared to other MOFs. In particular, they also exhibit a high affinity towards the diclofenac molecule

as observed through the calculation between the Langmuir constant and the maximum adsorption capacity. In conjunction with their ability to be reused after the regeneration process takes place, this then indicates that all the free-base porphyrins Zr-MOFs might be promising to be applied in real conditions where the concentration of the diclofenac molecule is usually relatively low.

Data availability

Author contributions

Nicholaus Prasetya: conceptualization, methodology, software, validation, formal analysis, investigation, data curation, writing – original draft, writing – reviewing & editing, visualization, project administration, funding acquisition. Christof Wöll: conceptualization, resources, supervision, writing – reviewing & editing, project administration, funding acquisition.

Conflicts of interest

There are no conflicts to declare.

Acknowledgements

Notes and references

1 Q. Shi, Y. Xiong, P. Kaur, N. D. Sy and J. Gan, *Sci. Total Environ.*, 2022, **814**, 152527.

2 E. Prásková, S. Štěpánová, L. Chromcová, L. Plhalová, E. Voslářová, V. Pištěková, M. Prokeš and Z. Svobodová, *Acta Vet. Brno*, 2013, **82**, 343–347.

3 I. Y. López-Pacheco, A. Silva-Núñez, C. Salinas-Salazar, A. Arévalo-Gallegos, L. A. Lizarazo-Holguin, D. Barceló, H. M. Iqbal and R. Parra-Saldívar, *Sci. Total Environ.*, 2019, **690**, 1068–1088.

4 H. N. Hong, H. N. Kim, K. S. Park, S.-K. Lee and M. B. Gu, *Chemosphere*, 2007, **67**, 2115–2121.

5 L. Lonappan, S. K. Brar, R. K. Das, M. Verma and R. Y. Surampalli, *Environ. Int.*, 2016, **96**, 127–138.

6 P. McGettigan and D. Henry, *PLoS Med.*, 2013, **10**, e1001388.

7 G. E. Swan, R. Cuthbert, M. Quevedo, R. E. Green, D. J. Pain, P. Bartels, A. A. Cunningham, N. Duncan, A. A. Meharg and J. Lindsay Oaks, *Biol. Lett.*, 2006, **2**, 279–282.

8 T. H. Galligan, J. W. Mallord, V. M. Prakash, K. P. Bhusal, A. S. Alam, F. M. Anthony, R. Dave, A. Dube, K. Shastri and Y. Kumar, *Bird Conserv. Int.*, 2021, **31**, 337–353.

9 Y. Liu, L. Wang, B. Pan, C. Wang, S. Bao and X. Nie, *Aquat. Toxicol.*, 2017, **183**, 104–113.

10 A. Peters, M. Crane, G. Merrington and J. Ryan, *Environ. Sci. Eur.*, 2022, **34**, 1–16.

11 B. N. Bhadra, P. W. Seo and S. H. Jhung, *Chem. Eng. J.*, 2016, **301**, 27–34.

12 F. M. O. Medina, M. B. Aguiar, M. E. Parolo and M. J. Avena, *J. Environ. Manage.*, 2021, **278**, 111523.

13 B. Y. Z. Hiew, L. Y. Lee, K. C. Lai, S. Gan, S. Thangalazhy-Gopakumar, G.-T. Pan and T. C.-K. Yang, *Environ. Res.*, 2019, **168**, 241–253.

14 H. Mahmoodi, M. Fattahi and M. Motevassel, *RSC Adv.*, 2021, **11**, 36289–36304.

15 M. Barczak, M. Wierzbicka and P. Borowski, *Microporous Mesoporous Mater.*, 2018, **264**, 254–264.

16 J.-K. Kang, Y.-G. Kim, S.-C. Lee, H.-Y. Jang, S.-H. Yoo and S.-B. Kim, *Microporous Mesoporous Mater.*, 2021, **328**, 111497.

17 K. Sun, Y. Shi, X. Wang and Z. Li, *J. Hazard. Mater.*, 2017, **323**, 584–592.

18 J. J. M. Garcia, J. A. P. Nuñez, H. S. Salapare III and M. R. Vasquez Jr, *Results Phys.*, 2019, **15**, 102629.

19 H. Yuan, J. Liu, X. Zhang, L. Chen, Q. Zhang and L. Ma, *J. Cleaner Prod.*, 2023, 135845.

20 K. Poonia, S. Patial, P. Raizada, T. Ahamad, A. A. P. Khan, Q. Van Le, V.-H. Nguyen, C. M. Hussain and P. Singh, *Environ. Res.*, 2023, 115349.

21 S. Nagappan, M. Duraivel, V. Elayappan, N. Muthuchamy, B. Mohan, A. Dhakshinamoorthy, K. Prabakar, J.-M. Lee and K. H. Park, *Energy Technol.*, 2023, **11**, 2201200.

22 B. Wang, X.-L. Lv, D. Feng, L.-H. Xie, J. Zhang, M. Li, Y. Xie, J.-R. Li and H.-C. Zhou, *J. Am. Chem. Soc.*, 2016, **138**, 6204–6216.

23 M.-M. Xu, Q. Chen, L.-H. Xie and J.-R. Li, *Coord. Chem. Rev.*, 2020, **421**, 213421.

24 N. Prasetya, I. G. Wenten, M. Franzreb and C. Wöll, *Coord. Chem. Rev.*, 2023, **475**, 214877.

25 Z. Hasan, N. A. Khan and S. H. Jhung, *Chem. Eng. J.*, 2016, **284**, 1406–1413.

26 N. Crespí Sánchez, G. Turnes Palomino and C. Palomino Cabello, *Microporous Mesoporous Mater.*, 2023, **348**, 112398.

27 S. Zhuang, R. Cheng and J. Wang, *Chem. Eng. J.*, 2019, **359**, 354–362.

28 N. Prasetya and K. Li, *Chem. Eng. J.*, 2021, **417**, 129216.

29 N. Prasetya and K. Li, *Sep. Purif. Technol.*, 2022, 122024.

30 B. N. Bhadra, I. Ahmed, S. Kim and S. H. Jhung, *Chem. Eng. J.*, 2017, **314**, 50–58.

31 S. Zhuang, Y. Liu and J. Wang, *Environ. Pollut.*, 2019, **253**, 616–624.

32 K. Yu, I. Ahmed, D.-I. Won, W. I. Lee and W.-S. Ahn, *Chemosphere*, 2020, **250**, 126133.

33 P. Deria, D. A. Gómez-Gualdrón, I. Hod, R. Q. Snurr, J. T. Hupp and O. K. Farha, *J. Am. Chem. Soc.*, 2016, **138**, 14449–14457.

34 W. Morris, B. Volosskiy, S. Demir, F. Gándara, P. L. McGrier, H. Furukawa, D. Cascio, J. F. Stoddart and O. M. Yaghi, *Inorg. Chem.*, 2012, **51**, 6443–6445.

35 X. Gong, H. Noh, N. C. Gianneschi and O. K. Farha, *J. Am. Chem. Soc.*, 2019, **141**, 6146–6151.

36 Y.-H. Wang, C.-H. Chuang, T.-A. Chiu, C.-W. Kung and W.-Y. Yu, *J. Phys. Chem. C*, 2020, **124**, 12521–12530.

37 K. Yu, D.-I. Won, W. I. Lee and W.-S. Ahn, *Korean J. Chem. Eng.*, 2021, **38**, 653–673.

38 S. M. Shaikh, P. M. Usov, J. Zhu, M. Cai, J. Alatis and A. J. Morris, *Inorg. Chem.*, 2019, **58**, 5145–5153.

39 C. Koschnick, R. Stäglich, T. Scholz, M. W. Terban, A. von Mankowski, G. Savasci, F. Binder, A. Schökel, M. Etter and J. Nuss, *Nat. Commun.*, 2021, **12**, 3099.

40 K. I. Hadjiivanov, D. A. Panayotov, M. Y. Mihaylov, E. Z. Ivanova, K. K. Chakarova, S. M. Andonova and N. L. Drenchev, *Chem. Rev.*, 2020, **121**, 1286–1424.

41 M. C. So, S. Jin, H.-J. Son, G. P. Wiederrecht, O. K. Farha and J. T. Hupp, *J. Am. Chem. Soc.*, 2013, **135**, 15698–15701.

42 E. D. Revellame, D. L. Fortela, W. Sharp, R. Hernandez and M. E. Zappi, *Cleaner Eng Technol.*, 2020, **1**, 100032.

43 H. A. Younes, M. Taha, R. Mahmoud, H. M. Mahmoud and R. M. Abdelhameed, *J. Colloid Interface Sci.*, 2022, **607**, 334–346.

44 C. Yao and T. Chen, *Chem. Eng. Res. Des.*, 2017, **119**, 87–92.

45 R. M. Viegas, M. Campinas, H. Costa and M. J. Rosa, *Adsorption*, 2014, **20**, 737–746.

46 G. Boyd, A. W. Adamson and L. Myers Jr, *J. Am. Chem. Soc.*, 1947, **69**, 2836–2848.

47 W. J. Weber Jr and J. C. Morris, *J. Sanit. Eng. Div., Am. Soc. Civ. Eng.*, 1963, **89**, 31–59.

48 L. Heinke, Z. Gu and C. Wöll, *Nat. Commun.*, 2014, **5**, 4562.

49 X. Zheng, J. Wang, X. Xue, W. Liu, Y. Kong, R. Cheng and D. Yuan, *Environ. Sci. Pollut. Res.*, 2018, **25**, 31705–31717.

50 H. C. Streit, M. Adlung, O. Shekhah, X. Stammer, H. K. Arslan, O. Zybaylo, T. Ladnorg, H. Gliemann, M. Franzreb and C. Wöll, *ChemPhysChem*, 2012, **13**, 2699–2702.

51 J. Janićijević, D. Krajišnik, B. Čalija, B. N. Vasiljević, V. Dobričić, A. Daković, M. D. Antonijević and J. Milić, *Int. J. Pharm.*, 2015, **496**, 466–474.

52 A. Karami, R. Sabouni and M. Ghommem, *J. Mol. Liq.*, 2020, **305**, 112808.